Original Article

Decrement Evoked Potential Mapping
Basis of a Mechanistic Strategy for Ventricular Tachycardia Ablation

Nicholas Jackson, MBBS; Sigfus Gizurarson, MD, PhD; Karthik Viswanathan, MD; Benjamin King, MBBS; Stephane Massé, MASc; Marjan Kusha, MEng; Andreu Porta-Sanchez, MD; John Roshan Jacob, MD; Fakhar Khan, MD; Moloy Das, MD; Andrew C.T. Ha, MD; Ali Pashaei, PhD; Edward Vigmond, PhD; Eugene Downar, MD; Kumaraswamy Nanthakumar, MD

Background—Substrate-based mapping for ventricular tachycardia (VT) ablation is hampered by its inability to determine critical sites of the VT circuit. We hypothesized that those potentials, which delay with a decremental extrastimulus (decrement evoked potentials or DEEPs), are more likely to colocalize with the diastolic pathways of VT circuits.

Methods and Results—DEEPs were identified in intraoperative left ventricular maps from 6 patients with ischemic cardiomyopathy (total 9 VTs) and were compared with late potential (LP) and activation maps of the diastolic pathway for each VT. Mathematical modeling was also used to further validate and elucidate the mechanisms of DEEP mapping. All patients demonstrated regions of DEEPs and LPs. The mean endocardial surface area of these potentials was 18±4% and 21±6%, respectively (P=0.13). The mean sensitivity for identifying the diastolic pathway in VT was 50±23% for DEEPs and 36±32% for LPs (P=0.31). The mean specificity was 43±23% versus 20±8% for DEEP and LP mapping, respectively (P=0.031). The electrograms that displayed the greatest decrement in each case had a sensitivity and specificity for the VT isthmus of 29±10% and 95±1%, respectively. Mathematical modeling studies recapitulated DEEPs at the VT isthmus and demonstrated their role in VT initiation with a critical degree of decrement.

Conclusions—In this preliminary study, DEEP mapping was more specific than LP mapping for identifying the critical targets of VT ablation. The mechanism of DEEPs relates to conduction velocity restitution magnified by zigzag conduction within scar channels. **(*Circ Arrhythm Electrophysiol*. 2015;8:1433-1442. DOI: 10.1161/CIRCEP.115.003083.)**

Key Words: cardiomyopathies ■ catheter ablation ■ evoked potentials ■ heart ventricles ■ tachycardia, ventricular

Catheter ablation of ventricular tachycardia (VT) is an important treatment to reduce symptoms and defibrillator shocks in patients with heart disease.[1] In high-risk patients referred for VT ablation and in patients with VT storm, successful ablation has also been associated with improved survival.[2,3] Activation mapping for VT may be the gold standard for identifying the diastolic pathway and critical isthmus, however, it is not possible in cases of hemodynamically unstable VT or where VT is not inducible. Substrate-based mapping and ablation during sinus rhythm or ventricular pacing has therefore become a common strategy in the current era of VT ablation.[4] The targets of substrate-based ablation are subjective and evolving, however, and research is ongoing into how the proposed targets can be linked to the mechanisms of initiation and maintenance of VT.[4–10]

Optimally, the ablation targets identified with substrate mapping would participate in the initiation of or act as diastolic channels for the maintenance of reentrant circuits in VT. Given that conduction delay and unidirectional block are essential for the initiation and maintenance of reentry,[11] identifying these regions by their electrophysiological behavior would be of value in VT mapping.

We hypothesized that ventricular electrograms, which displayed decremental conduction (decrement evoked potentials or DEEPs), are more likely to participate in reentrant VT circuits than conventional substrate ablation targets. We tested this concept with a rigorous reference standard where the entire reentrant path during VT had been mapped simultaneously by intraoperative array mapping. This diastolic pathway was then related to simultaneous mapping of the same region during pacing with extrastimuli to evoke decremental conduction. We also validated our preliminary derivations on DEEP mapping with mathematical modeling and elucidated the mechanism of the participation of these potentials in the initiation and maintenance of VT.

Received January 9, 2015; accepted October 13, 2015.

From the Toronto General Hospital, Toronto, Ontario, Canada (N.J., S.G., K.V., B.K., S.M., M.K., A.P.-S., J.R.J., F.K., M.D., A.C.T.H., E.D., K.N.); Laboratory IMB, University of Bordeaux, Talence, France (A.P., E.V.); and LIRYC Cardiac Electrophysiology and Heart Modelling Institute, University of Bordeaux Foundation, Pessac, France (A.P., E.V.).

Correspondence to Kumaraswamy Nanthakumar, MD, Division of Cardiology, University Health Network, Toronto General Hospital, 150 Gerrard St W, GW3-522, Toronto, Ontario M5G 2C4, Canada. E-mail kumar.nanthakumar@uhn.ca or Nicholas Jackson, MBBS, Toronto General Hospital, Toronto, Ontario, Canada. E-mail jackson193@gmail.com

WHAT IS KNOWN

- Substrate based mapping for VT ablation using late potentials, local abnormal electrograms and pace mapping for scar dechanneling and homogenization has become part of the empirical approach.
- These strategies, however, have a low specificity for identifying the specific VT isthmus and they assume fixed barriers of scar and do not detect evidence of functional conduction block and delay that can also determine reentry.

WHAT THE STUDY ADDS

- This study analysed operative mapping data finding that local abnormal potentials which delay with a decremental extrastimulus (decrement evoked potentials or DEEPs) appear to be relatively specific for a VT isthmus.
- In a mathematical model the effect of conduction velocity restitution following extrastimuli was magnified by zigzag conduction within the scar tissue channel producing sufficient delay for reentry involving DEEP regions.

Methods

Approval for this study was obtained from our local institutional review committee. To assess the efficacy of DEEP mapping, we retrospectively analyzed the results of intraoperative mapping from 6 patients with a history of remote myocardial infarction and recurrent reentrant VT, which was refractory to medical therapy. After this, we used the Ten Tusscher human ionic model,[12] with a labyrinthine-conducting channel to mathematically model and derive the relationship of DEEPs with the diastolic isthmus in VT.

Intraoperative Mapping System

The techniques for intraoperative mapping[13,14] and patient follow-up[15] have been described in detail previously. Briefly, the heart was accessed via a median sternotomy, and cardiopulmonary bypass was initiated. Mapping was performed with a custom-made 112-electrode endocardial balloon, which was inserted into the left ventricular cavity via a left atriotomy and filled with saline to ensure adequate endocardial contact. Each electrode was made of two 2-mm diameter silver beads separated by 1 mm from which bipolar electrograms were recorded.

The bipolar electrograms were amplified, filtered, and recorded using a custom-made mapping system from our institution that has been previously described.[13,14] Filter settings were 28 to 750 Hz for bipolar electrograms, with signal amplification of ≤20 000 times. This small interelectrode distance between the bipolar electrodes allowed measurements of small local potentials in the range of 50 to 100 μV. High gains were chosen to reveal small diastolic/local abnormal potentials for optimal mapping of diastolic pathways. Electrograms were then digitized at 2 kilosamples/s and stored on a computer for later offline analysis.

Mapping and Ablation protocol

Induction of VT was performed with right ventricular (RV) pacing by the introduction of premature extrastimuli (S2–S4) after a paced train (S1) at a basic cycle length of 400 to 600 ms. The clinical relevance of each induced VT was determined by comparison with previously recorded episodes of VT from the patients with 12-lead ECGs. Surgical cryoablation was then performed at areas considered to be critical for VT maintenance based on activation mapping (as the DEEP method was applied retrospectively).

Substrate Mapping

Two-dimensional color-coded endocardial maps were created from the bipolar electrogram data recorded during RV pacing. Maps are displayed as bulls-eye plots with the apex in the center and the basal left ventricle at the periphery. Electrode row 1 was aligned with the anterior intraventricular groove (the course of the left anterior descending artery), and the rows subsequently continue clockwise to the lateral, inferior, and septal endocardial walls of the left ventricle.

Four types of maps were created for each patient as follows. Voltage (scar) maps were created during RV pacing, where a threshold of ≤0.5 mV was used to define scar.[16] Late potential (LP) maps were created during RV pacing by tagging the latest sharp, near-field potential occurring after the end of the paced QRS complex (Figure 1).

DEEP Mapping

The basis of this mapping technique was to identify those isolated near-field potentials that delayed in timing with a single extrastimulus. We refer to these as DEEPs because they are identified (evoked) by a decremental extrastimulus. During programmed ventricular stimulation, we annotated the latest sharp, near-field component of the bipolar signals during the pacing train and on the first extrastimulus. The change in timing of the isolated potentials during the pacing train and the extrastimulus with reference to the onset of the QRS on the surface ECG denoted the degree of delay. By measuring timing relative to the onset of the QRS, this corrected for any local latency that may have occurred with closely coupled extrastimuli at the RV pacing catheter (Figure 1).

Whenever a LP or fractionated potential was identified during substrate mapping, a pacing train was performed at 600 ms with a single extrastimulus delivered at the ventricular effective refractory period (VERP) +20 ms (stimulation was bipolar at just above threshold value). If the local potential on the mapping catheter delayed, this would be annotated as a DEEP. If the potential blocked, then the extrastimulus could be repeated with a longer coupling interval (ie, VERP +40 ms). To minimize interobserver error when determining the onset of near-field activation, a minimum delay of 10 ms was required for an electrogram (EGM) to be categorized as DEEP. The timing windows for the DEEP maps were then manually set for each patient so that all points with significant delay (≥10 ms) were displayed.

Diastolic Activation Map During VT

After induction of VT, diastole was defined as the time from the end of all QRS complexes on the surface ECG to the beginning of the earliest QRS complex in the applicable leads. Hence, all areas with electrical activity during diastole were displayed, including activation in all bystander areas. Care was taken to annotate only true near-field diastolic activity based on sharp near-field EGMs displaying a high dV/dt. Based on prior studies[17] that the true exit from the diastolic channel into rapid radial spread across the myocardium occurs significantly earlier (30–80 ms) than the onset of the surface QRS, we chose to limit our attention to the middle 70% of the diastolic period (mid-diastolic activation period). This would exclude postexit and preentrance site activations during ventricular diastole.

Pacing maneuvers were not used to discriminate bystander sites from isthmus sites. Instead, because the entire endocardium was mapped simultaneously, the isthmus was defined as the shortest possible diastolic return pathway by examining the activation sequence on adjacent bipoles. Adjacent bystanders were identified as there was no progression of local activation on the surrounding electrodes, indicating a dead-end to conduction.[18]

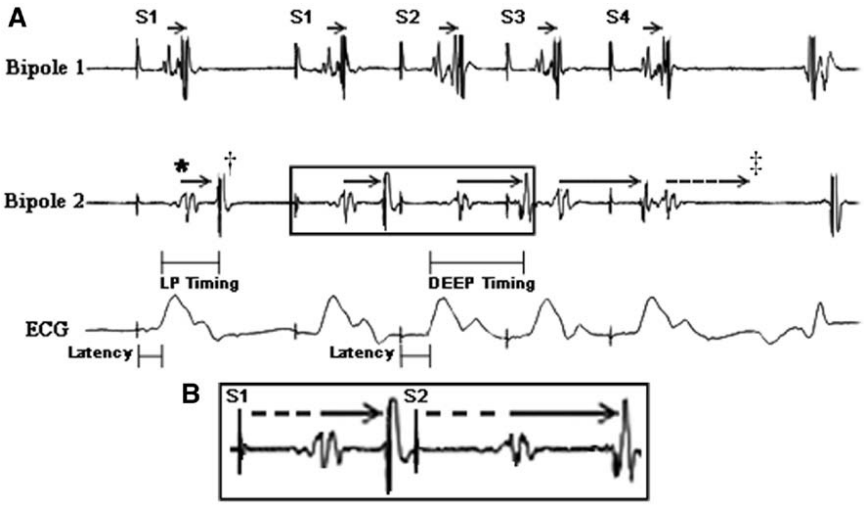

Figure 1. A, Recordings from 2 bipoles close to a ventricular tachycardia exit site during right ventricular pacing. The surface ECG is shown for reference, and pacing stimulus artifacts are indicated. The last 2 beats of the pacing train are followed by 3 extrastimuli. After the first pacing spike on bipole 2, a low-frequency far-field ventricular ECG (electrogram [EGM]) is seen (*) followed by a high-frequency near-field EGM (†), which constitutes a late potential (LP). How the timing of this LP was annotated for LP maps is shown. The high-frequency local potential on bipole 2 demonstrates significant delay followed by block with the extrastimuli (‡); however, the local EGM on bipole 1 retains relatively fixed timing and does not block. The timing of decrement evoked potentials (DEEPs) for DEEP maps were annotated from the beginning of the surface QRS to correct for latency (as shown). **B**, The last beat from the pacing train and the first extrastimulus. Clear delay of the near-field potential is seen at this site indicating the presence of a DEEP.

Relating LP and DEEP Mapping to Mid-Diastolic Activation During VT

As previously described, the mid-diastolic segment (70%) of the VT circuit was annotated on all activation maps. The number and position of those bipoles that demonstrated activation during mid-diastole were then compared with the bipoles demonstrating DEEPs and LPs, respectively. Those bipoles showing LPs were also correlated to the regions of DEEPs and vice versa. We also adjusted the voltage on our intraoperative scar maps to look for channels within scar tissue that harbored LPs similar to the protocol performed by Mountantonakis et al[19] and analyzed the sensitivity and specificity of these potentials for identifying the diastolic isthmus.

Modeling Methods

To further validate the DEEP concept and study the mechanisms of decremental conduction in scar channels, a modeling study was performed. Simulations were performed on a 4×4 cm tissue with sealed edges. A scar measuring 2×2 cm was placed in the center of the tissue that was implemented as an unexcitable zone with a single labyrinthine-conducting channel. The major lengths of the channel were oriented along the fiber direction with switchbacks across the transverse direction.[20] Channels were 1 mm wide and ranged from 14.4 to 25.4 cm long. A wave diode (a channel that allows wavefront propagation in only 1 direction) was placed at the exit point of the channel by creating a step reduction in width of the channel to 300 μm for 1 mm and reducing the tissue conductivity of the left half in this portion of the strand. Activity could conduct to the right but not to the left, thereby creating unidirectional block.

Unipolar and bipolar electrograms were recreated by computing the transmembrane currents and calculating the potentials produced by these currents. Electrodes were 1 mm in diameter (placed 500 μm off the surface), and electrode measurements were extracellular potentials averaged over the surface of the electrode. A second sheet of tissue with no scar was placed exactly below the original for far-field signal generation, and any stimulus applied was through both sheets. Far-field activation was determined by the minimum negative derivative of the unipolar electrogram, whereas local activation was measured as the maximum amplitude deflection of a bipole oriented in the cross-fiber direction. The system was solved using a monodomain formulation and the Cardiac Arrhythmia Research Package (CARP) simulator. The tissue was discretized at 150 μm and solved with a time step of 25 μs. The Ten Tusscher[12] human ionic model was used. Ionic model and conductivity parameters were the same for the channel as for the normal myocardium.

Statistical Analysis

The endocardial surface areas of LPs and DEEPs were calculated by adding up the total number of bipoles displaying these potentials and expressing them as a percentage out of 112 (the total number

Table. Baseline Characteristics of the Patients From the Intraoperative Mapping Study

Patient No.	Sex	Cardiomyopathy Type	Region of Scar	VT Cycle Length, ms	Area of LPs, %	Area of DEEPs, %
1	Male	ICM	Inferior	320, 300	14.3	17.0
2	Male	ICM	Anterior	320	17.0	13.4
3	Male	ICM	Inferolateral	220, 200	18.8	17.0
4	Male	ICM	Anteroseptal	360	22.3	15.2
5	Male	ICM	Inferoapical	260, 300	24.1	23.2
6	Male	ICM	Apical	390	30.4	19.6

The percentage of the endocardial area on array mapping that consisted of LPs and DEEPs are shown as a percentage of the total electrodes on the array. DEEPs indicates decrement evoked potentials; ICM, ischemic cardiomyopathy; LPs, late potentials; and VT, ventricular tachycardia.

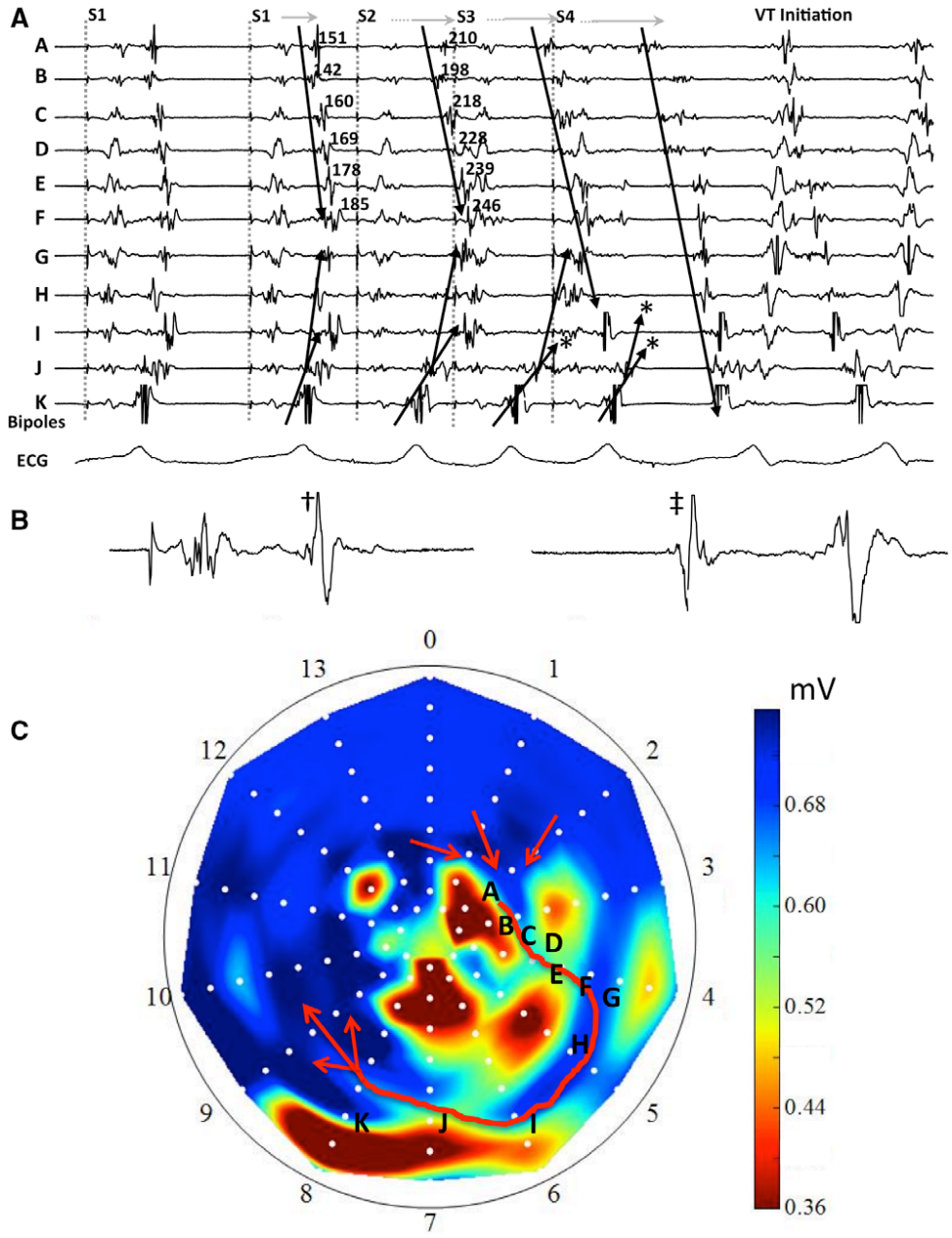

Figure 2. A, An example of decremental conduction, unidirectional block, and induction of ventricular tachycardia (VT). Bipoles A to K are located sequentially within the diastolic pathway of the VT circuit. During right ventricular pacing (S1), local abnormal potentials can be seen on bipoles F, I, and J, and these would be annotated when creating a late potential (LP) map. With the introduction of a premature stimulus (S2), there is marked delay of the local electrograms across all bipoles from A to J. With S3, there is block (*) of the local potential on bipole I, and subsequently with S4, there is block (*) at the VT exit site (bipole J). Block at the VT exit site and conduction delay through the entrance to the diastolic isthmus sets up the environment for the reentrant circuit to begin. Bipoles A to J then span the entire diastolic limb of the VT circuit. This VT initiation demonstrates the concept of decrement evoked potential mapping; that conduction delay precedes unidirectional block and the initiation of tachycardia at critical points in the VT circuit. Measurements on S1 and S2 from bipoles A to F show the degree of delay of the local potential from QRS onset in milliseconds. Substantial delay occurs at bipoles A and B with the extrastimulus, and minimal additional decrement occurs further down the isthmus from bipoles C to F. **B**, An enlarged image of bipole H from **A**. The split potential following S1 is enlarged to clearly show the polarity of the local component (†). With S4, block to bipole H occurs through the exit site of the VT isthmus, and this bipole is subsequently activated via the VT entrance site from the opposite direction. This change in direction of activation leads to an exact polarity change in the local electrogram (‡). **C**, A corresponding scar map of the LV with the voltage scale on the **right**. Apical electrodes are at the center, basal electrodes at the periphery, and spline 0 is oriented to the anterior interventricular groove. Heterogeneous scar is found at the apex and extends to the inferobasal region. The diastolic pathway of the VT shown in Figure 2A is drawn (red arrow), and the corresponding electrodes are labeled.

of bipoles). The sensitivity and specificity of the LP and DEEP maps were calculated individually for each VT and expressed as the mean±SD. Where multiple VTs occurred in the same patient, these values were averaged to account for intrasubject correlation. Comparison was made using a Wilcoxon signed-rank test. A P value of <0.05 was considered statistically significant.

Results

Simultaneous Global Mapping Study

Nine VTs from 6 patients (3 patients with 2 VTs each) were analyzed. Clinical characteristics and tachycardia cycle lengths from each patient/VT are shown in Table.

Connecting Decrement to Unidirectional Block and VT

Both Figures 1 and 2 demonstrate LPs that delay when an extrastimulus is delivered from 2 different cases. In both cases, 3 extrastimuli are given, which result in progressively greater delay of multiple local potentials, followed by block in some of those LPs. In both cases, delay of the local potentials occurs over and above the latency caused by premature RV stimuli. In the case of Figure 2, this delay and block result in the initiation of VT.

Figure 2A shows significant delay in the timing of local activation at bipoles A to F, whereas local activation at bipole K does not delay. Figure 2C demonstrates that bipole K is likely to be just beyond the exit site of the VT isthmus within healthy tissue, explaining why this potential does not delay (or display decremental conduction). As the RV pacing wavefront travels across the ventricular septum during the pacing train, it invades the diastolic isthmus from both ends (both the entrance and the eventual exit site of the VT isthmus). Significant decrement begins at bipoles A and B with the extrastimuli, and although significant decrement is seen at bipoles C to F, no additional decrement seems to occur between bipoles C to F themselves. Rather they appear to decrement as a result of the sum of all the preceding decrement in the circuit up to that point (most of which occurred around bipoles A and B). The local potentials also delay at bipoles G to J, until block occurs between bipoles I and J on the third extrastimulus and instead of wave fronts colliding at bipoles G and H, these electrode pairs become activated from the opposite direction and VT initiates. Figure 2B demonstrates the reversal of electrogram polarity at bipole H with VT initiation because it is now activated by a wavefront traveling in the opposite direction. In 4 of the 6 VTs that were initiated with a single stable morphology, this phenomenon preceded VT onset.

In Figure 2, the diastolic pathway of the VT is delineated by electrodes A through J (with A defining the entrance and J the exit). The local electrograms at all of these electrodes show delay and would be classified as points of interest by DEEP mapping. Converse to this, LPs are only seen at bipoles F, I, and J during the pacing train. Hence, this figure illustrates greater sensitivity for DEEP mapping in identifying the diastolic pathway of this VT over conventional LP mapping. This same diastolic pathway is used in the opposite direction to produce a second VT morphology in Figure 3. This VT was induced during an attempt to overdrive pace the previous VT and demonstrates how DEEP mapping may identify points that are critical to more than 1 ventricular tachycardia morphology or circuit.

Substrate and Activation Maps

Areas displaying diastolic activity were found within areas of scar or scar borders in all patients. In all mapped VTs, at least two thirds of the diastolic pathway was mapped, and on average the diastolic pathway of VT encompassed 18.8±9.7% of the total endocardial surface area. Substrate and activation maps are shown from a different simultaneous global mapping case in Figure 4A. The diastolic activation map seems to correspond with the voltage (scar) map to demonstrate a diastolic isthmus that travels between the 2 regions of dense scar at the mid anterolateral endocardium (white arrows). The DEEP map colocalizes with the entrance and exit portions of this diastolic channel; however, the LP map only identifies potentials in scar border zones at the apex, away from the diastolic circuit.

DEEPs Colocalize With the Diastolic Pathway in VT

All patients demonstrated areas of LPs and DEEPs, with an area of 21±6% and 18±4%, respectively, P=0.13. There was overlap in areas demonstrating both LPs and DEEPs at 7±2% of the endocardial surface. Areas with LPs also demonstrated DEEPs in 37±13% of electrode pairs, and DEEPs similarly originated from LPs at 45±19% of electrodes. The sensitivity of substrate mapping for identifying areas with mid-diastolic activation was 50±23% for DEEP mapping and 36±32% for LP mapping (P=0.31). However, the specificity of DEEP mapping (43±23%) was significantly higher than that of LP mapping (20±8%, P=0.031).

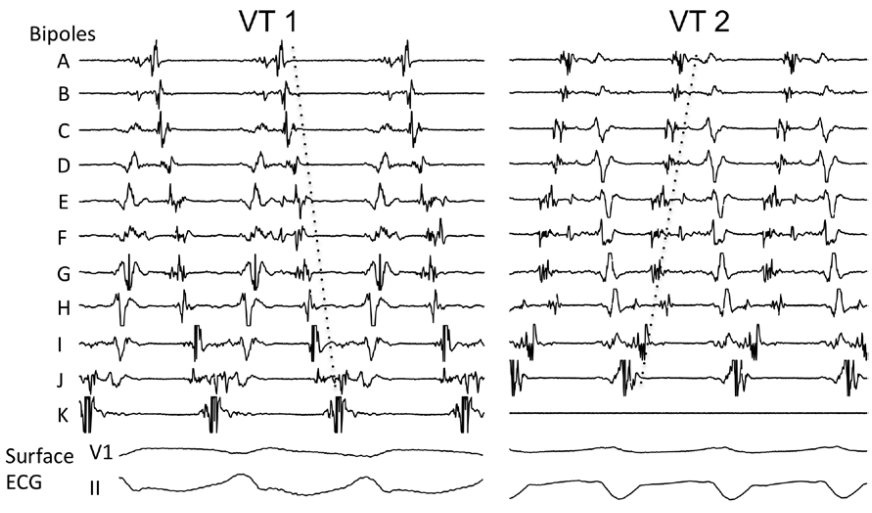

Figure 3. Electrograms during ventricular tachycardia (VT) from the same patient with the same anatomic position of the array as shown in Figure 2. **Left**, VT is seen with an inferior axis (VT-1) with diastolic activation running from bipole A (entry) through mid-diastole (E–G) and finally exiting close to bipole J. After attempted, pace termination VT-2 was induced (**right**) with an approximately opposite diastolic activation pattern and a superior axis. The cycle lengths both approximate each other suggesting VT-2 uses the identical diastolic pathway to VT-1 but in the opposite direction. This figure demonstrates how regions with decrement evoked potentials (DEEPs) can form the substrate for multiple VT morphologies and multiple variations of the same diastolic pathway.

When we examined the points that displayed the greatest decrement in each case (8 points per case), the sensitivity for identifying the diastolic isthmus was 29±10% (*P*=0.031 compared with all DEEPs), and the specificity was 95±1% (*P*=0.031 compared with all DEEPs). The mean amount of decrement (adjusted for latency) seen at these points was 27±13 ms. The mean sensitivity of LPs within scar channels was 34.3% (*P*=0.25 compared with all DEEPs), and the specificity was 91.9% (*P*=0.1 compared with all DEEPs) for identifying the VT isthmus in this cohort. Only 3 of the 6 intraoperative cases in this study, however, displayed LP-positive scar tissue channels. The likelihood ratios for identifying the diastolic isthmus for these 4 methods are detailed in Figure 4B.

Modeling Study

One edge of the tissue was stimulated to create a planar wavefront at a constant S1 cycle length of 500 ms. Regardless of the

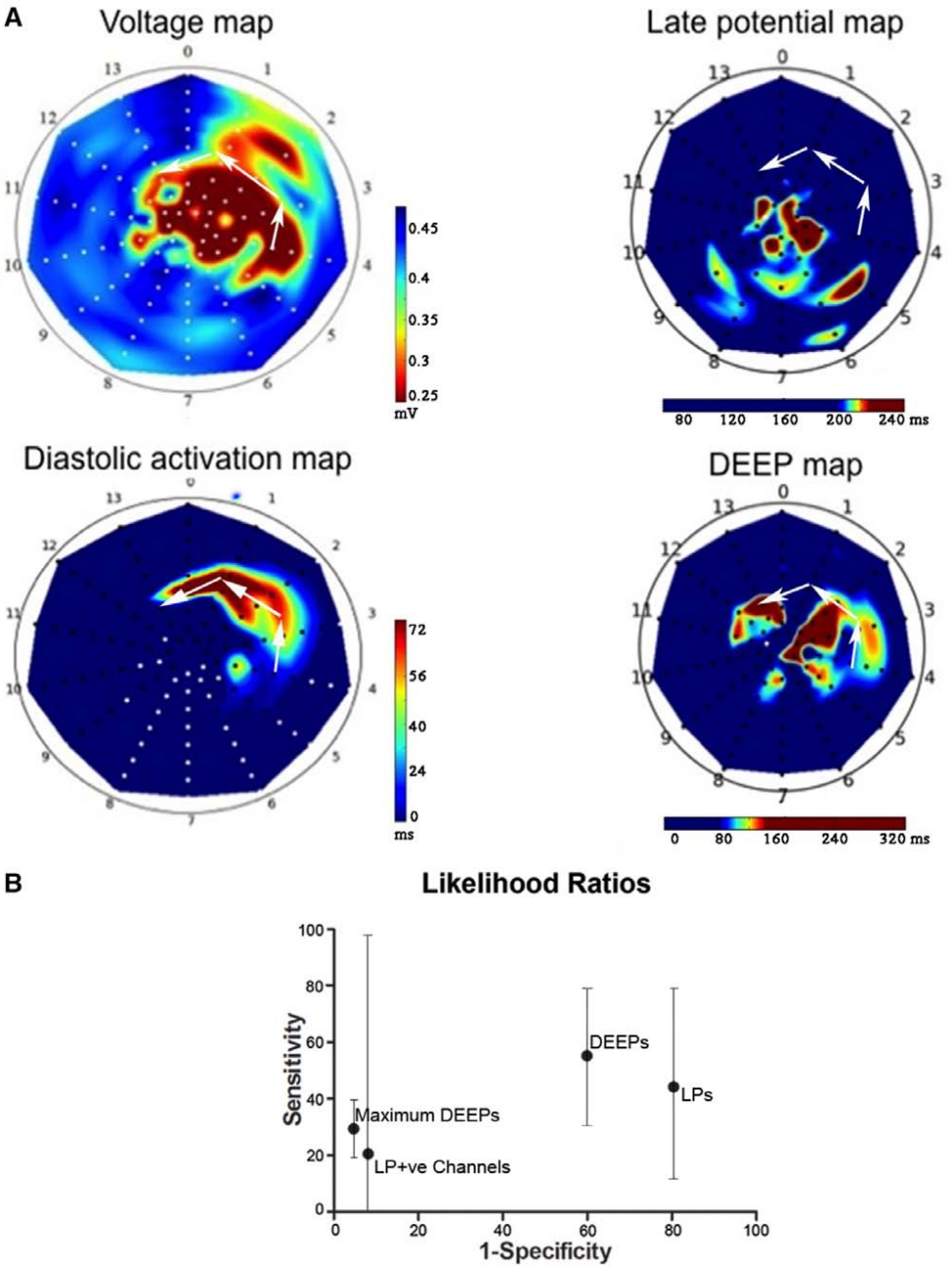

Figure 4. A, An example of 4 different left ventricular (LV) endocardial maps from the same patient (apex at the center and base at the periphery). The voltage map shows an area of apical scar with extension to the anterolateral walls. The diastolic channel on the activation map is found at the anterolateral wall in a region with borderline voltages sandwiched between dense scar (white arrows define the diastolic pathway). The late potential map identifies electrograms at the LV apex around scar border zones that are remote from the diastolic pathway of the mapped ventricular tachycardia (VT). The decrement evoked potential (DEEP) map, however, corresponds to early and late isthmus sites; suggesting a greater specificity for identifying ablation targets in this VT. **B**, True-positive results plotted against false-positive results to generate likelihood ratios for late potentials (LPs; 0.54), DEEPs (0.92), LPs within scar channels (2.52), and points with the greatest decrement or maximum DEEPs (6.3) to identify the diastolic isthmus. The mean likelihood ratios are given above with the 95% confidence intervals on the figure.

direction of propagation, the wavefront entered the channel at one end but was blocked at the other end by the wave diode. Below a channel length of 25.4 cm, the wavefront would meet refractory tissue, as it exited the channel at the wave diode and be extinguished. If the channel was longer, the excitation wavefront would exit the scar and reenter the channel at the previous entry site.

We chose a channel length slightly shorter than that producing reentry and applied an S2 after a train of 4 S1 stimuli. In this case, the wavefront did not exit the channel during the pacing train but did exit after the S2 pulse. The S2 needed for reentry (adequate decrement) was dependent on the direction of the wavefront (being 260 ms with inferior stimulation or 310 ms from the sides of the tissue model). We then created a DEEP map that showed an increase in the degree of decrement along the length of the channel with the greatest value at the exit site.

The only factor in our model to account for decrement and delay was conduction velocity (CV) restitution. For this reason, we also examined the effect of reduced Na conductance in the channel (which is known to affect CV, see Figure 5C). The CV inside the scar channel was reduced, and the slope of the CV restitution curve was also mildly reduced (Figure 5C). Given the length of the scar channel, however, the wavefront transit time was still noticeably increased, irrespective of Na conductance.

Discussion

During simultaneous global intraoperative mapping, we found that potentials with decremental properties within scar or at scar border zones can identify targets for ablation that are more likely to participate in VT circuits than the targets of conventional substrate mapping. In this setting, the use of DEEP mapping identified the diastolic pathway with greater specificity than LP mapping. The primary advantage of DEEP mapping is to identify ablation targets without the need for VT induction and to identify specific targets in the diastolic pathway of the VT, which allows for a safer and more focused ablation strategy.

Prior studies suggest that at least 20% of the time patients have no inducible clinical tachycardia at the time of study.[6,7] Even when induced, factors such as hemodynamic compromise, lack of capture during entrainment, inability to delineate the entirety of the diastolic pathway,[21] and termination/conversion of tachycardia during entrainment limit the utility of activation mapping for VT ablation. Thus, the most frequent strategy currently used for VT ablation is a combination of activation and substrate mapping.[22,23]

Substrate mapping currently involves careful delineation of the scar and surrounding areas during sinus rhythm or ventricular pacing[24] to target sites of fractionated, double, or LPs. The identification of LPs or local abnormal ventricular activations (LAVAs) is subjective, and in some cases, scar border zones may be abundant with LAVA. This article deals with the issue of looking at LAVAs and determining which of these potentials is a physiologically meaningful target. Hence, the primary difference between this study and that by Jais et al[5] is that we attempted to refine the subset of LAVAs to those potentials that are more likely to participate in VT circuits and provide a more focused ablation strategy. Our study provides further evidence that the majority of LPs are not involved in

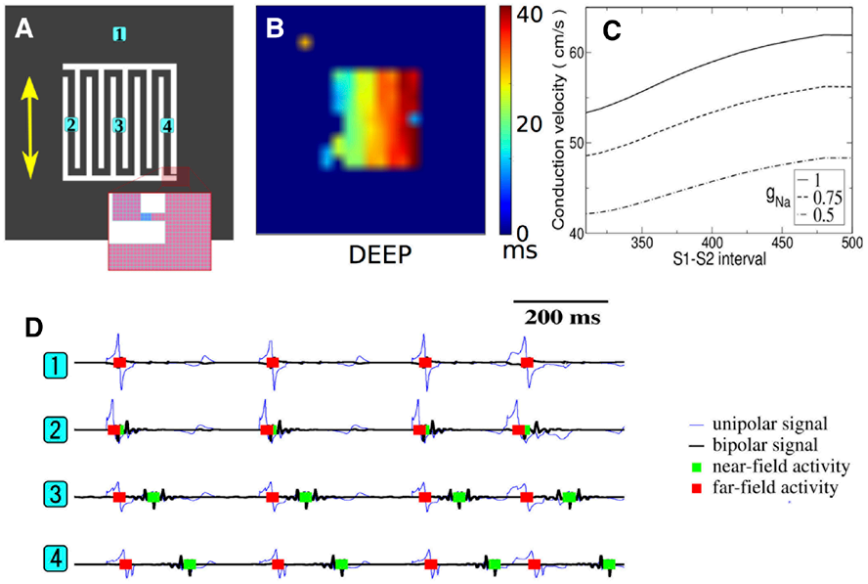

Figure 5. A, A model of myocardial tissue with scar. Normal myocardium is in black, and unexcitable tissue (scar) is white. The yellow arrow indicates fiber direction, and a wave diode (a channel that allows wavefront propagation in only one direction) is shown in detail at the bottom. Within the wave diode, pink squares represent myocardium with normal conductivity, blue squares have conductivity reduced to 25%, and white is unexcitable. **B**, The simulated decrement evoked potential map from left edge stimulation (there is progressively increasing delay of the local potential with progression further down the isthmus). **C**, Conduction velocity restitution curves measured inside the channel at location 3 for 3 levels of Na channel conductance (black lines). With decreasing Na channel conductance (simulating scar/abnormal tissue), there is a decrease in conduction velocity. **D**, Unipolar and bipolar electrograms measured at the locations indicated in **A** (locations 1, 2, 3, and 4). Three S1 pulses are shown (delivered along the left edge of the tissue model) followed by 1 S2 impulse. Delay of the near-field potential (green squares) is seen clearly at position 3 (mid isthmus) and is greatest at position 4 (close to the exit).

tachycardia circuits (specificity for LP mapping 20±8%) and is consistent with previous studies of substrate mapping.[19] When DEEPs with the greatest decrement were examined, the specificity for the diastolic isthmus was 95±1% in this study (with a likelihood ratio for identifying the diastolic isthmus of 6.3). This was similar to the specificity for LP positive scar channels in this study (91.9%), however, only 3 of the 6 intraoperative cases displayed LP-positive scar channels in this cohort. In the study by Mountantonakis et al,[19] 46% of patients had LP-positive scar channels, suggesting that this specific finding is only present around half the time.

Even when LPs are clearly visible beyond the QRS and sometimes well into diastole, these LPs may represent fixed delayed conduction into scarred myocardium. It is primarily the regions of the myocardium that display decremental conduction, however, which allows the time for blocked regions to recover excitability that can initiate reentry. Regions of the myocardium, where conduction blocks without adjacent delayed conduction, may not have sufficient excitable gap to initiate or sustain reentry. The concept of decrement preceding unidirectional block has been shown elegantly in atrial tissue sections. Lammers et al[11] used a rabbit model to show that regions, which demonstrated the greatest decrement, did indeed correlate with the sites of exit of reentrant tachycardia. This is consistent with our VT mapping and modeling data.

Improved sensitivity of DEEPs over LPs in some instances in the intraoperative study (although not statistically significant overall) may be because these abnormal potentials are hidden within the QRS or the far-field EGM at baseline. Local abnormal potentials (which represent small diastolic channels) may be difficult to see in the presence of a large far-field EGM. When they are stressed by a closely coupled extrastimulus, however, decremental conduction in these channels may delay this small diastolic potential so that its timing is well beyond the QRS or far-field EGM making it more evident.[5] The inability to identify the presence of these potential diastolic channels during fixed pacing is likely to be the reason for the improved sensitivity in some instances with DEEP mapping.

The concept of unidirectional block at the initiation of reentrant tachycardia is not new. Previous studies of postinfarct VT initiation mechanisms in both animals[25] and humans[26] have confirmed that VT induction is dependent on unidirectional block. Furthermore, it has been suggested that the site of unidirectional block may be close to the exit of a subsequently induced VT.[26] In this study, Figures 2 and 3 demonstrate how decrement can lead to different modes of VT initiation using the same diastolic path. In Figure 2C, if sufficiently delayed conduction occurred in an impulse traveling in the direction from bipoles K to A so that the myocardium was not refractory when the impulse exited at bipole A (assuming the diastolic isthmus had no retrograde invasion), then reentrant VT could be initiated where bipole A was the exit site (as in Figure 3). Conversely, in the example in Figure 2A, delay and then block occurs at bipoles I and J, so that these bipoles then become the exit site for VT. In this way, the directionality of the paced wavefront may affect the VT that is induced[27] and whether local potentials decrement or not. DEEP mapping requires further validation in other cardiomyopathy substrates and in atrial tachycardias, where decremental conduction, unidirectional block, and reentry are also common.

Some studies suggest that points of decrement in VT circuits are not within the protected isthmus itself but represent the points of wavefront turn around just proximal and distal to the true isthmus.[28] The degree of decrement seen may relate to the degree of wavefront curvature[29] or to the change in the direction of wavefront propagation relative to myocardial fiber orientation.[30] In our modeling study, a closer coupled extrastimulus was needed to initiate reentry when stimulation was performed inferiorly (so the wavefront travelled parallel to myocardial fiber orientation), as opposed to from the side of the model (with a perpendicularly oriented wavefront). In the surgical study, Figure 2A demonstrates that significant decrement is seen at bipoles A and B with an extrastimulus (entrance site), however, there is little additional decrement along the isthmus between bipoles C and F, consistent with this premise. Creating DEEP maps, however, displays the total amount of decrement in the circuit up to the bipole in question. In this way, midisthmus points will be annotated late on a DEEP map (signifying their importance) even when the greatest degree of decrement may be occurring just before or after the protected isthmus.

The reason for decremental conduction seen at DEEPs from our computer simulation was CV restitution. Consider a wavefront approaching a scar (as we have modeled) with an electrode at point 4 (Figure 5). Far-field activation is detected at point 4, as the wavefront travels through the adjacent healthy myocardium. Local activation at point 4 (near field), however, occurs significantly later because the wavefront from the initial stimulus has to travel a much greater distance through the zigzag-shaped scar channel. The time delay between the far-field and near-field electrograms will be relative to the distance through the scar channel to point 4 minus the distance through the myocardium to point 4, divided by the CV. At faster pacing rates, CV will slow, and further delay will be seen in the near-field signal with respect to the far-field signal, creating what we refer to as DEEPs. Accordingly, the greatest amount of delay was seen in DEEPs that were closest to the exit sites in our scar model (Figure 5D). DEEPs are seen best, where CV restitution leads to the greatest decrease in CV, explaining the mechanism by which DEEPs highlight reentrant pathways.

Pacing within regions of scarred myocardium and looking for a morphology match to the clinical VT and a long stimulus to QRS interval to identify the critical isthmus during substrate mapping has been used.[4–10] Both pace mapping and the DEEP method, however, will also identify bystander sites adjacent to the critical isthmus. In a study by Nayyar et al,[9] channels with a slower CV were more likely to be involved in VT circuits, although absolute CV measurements have significant limitations[9] and require relative measurements from multiple pacing sites. A further study suggests that the regions with the latest activation in sinus rhythm are infrequently associated with successful ablation sites, whereas slowly conducting regions that propagate into the latest zone of activation do correlate with successful ablation sites during VT.[31]

Limitations

This study primarily examined arrhythmias in patients with ischemic cardiomyopathy in the derivation set. Ideally, the efficacy of DEEP mapping and ablation should be tested in a prospective fashion with a clinical end point, such as recurrence of symptomatic VT or implantable defibrillator therapies. We are currently conducting this prospective clinical trial using contemporary electroanatomic mapping systems in the electrophysiology laboratory setting.

In the modeling study, we used a 2-dimensional (2D) model with a single-scar tissue channel that did not allow retrograde wavefront invasion because of the wave diode. This illustrates the role of DEEPs in reentry, however, it is an oversimplification from clinical practice, where scars are 3D, infarction is heterogeneous and multiple scar tissue channels may be seen.

Conclusions

DEEP mapping assesses the decremental properties of myocardial potentials and may provide a unique strategy for substrate-based VT ablation that is mechanistic. DEEP mapping identified the diastolic pathway of VT with greater specificity than LP mapping in the intraoperative part of this study. Mathematical modeling shows that the mechanism of DEEPs relates to CV restitution magnified by zigzag conduction in scar channels. This strategy provides a mechanistic framework for a more focused VT substrate ablation.

Sources of Funding

This study was funded by the Canadian Institutes of Health Research, grant no. PPP-133378 and an unrestricted grant by Ben Varadi.

Disclosures

K. Nanthakumar is a consultant for Biosense Webster and St. Jude Medical. S. Massé is a consultant for St. Jude Medical.

References

1. Natale A, Raviele A, Al-Ahmad A, Alfieri O, Aliot E, Almendral J, Breithardt G, Brugada J, Calkins H, Callans D, Cappato R, Camm JA, Della Bella P, Guiraudon GM, Haïssaguerre M, Hindricks G, Ho SY, Kuck KH, Marchlinski F, Packer DL, Prystowsky EN, Reddy VY, Ruskin N, Scanavacca M, Shivkumar K, Soejima K, Stevenson WJ, Themistoclakis S, Verma A, Wilber D; Venice Chart members. Venice Chart International Consensus document on ventricular tachycardia/ventricular fibrillation ablation. *J Cardiovasc Electrophysiol*. 2010;21:339–379. doi: 10.1111/j.1540-8167.2009.01686.x.
2. Carbucicchio C, Santamaria M, Trevisi N, Maccabelli G, Giraldi F, Fassini G, Riva S, Moltrasio M, Cireddu M, Veglia F, Della Bella P. Catheter ablation for the treatment of electrical storm in patients with implantable cardioverter-defibrillators: short- and long-term outcomes in a prospective single-center study. *Circulation*. 2008;117:462–469. doi: 10.1161/CIRCULATIONAHA.106.686534.
3. Della Bella P, Baratto F, Tsiachris D, Trevisi N, Vergara P, Bisceglia C, Petracca F, Carbucicchio C, Benussi S, Maisano F, Alfieri O, Pappalardo F, Zangrillo A, Maccabelli G. Management of ventricular tachycardia in the setting of a dedicated unit for the treatment of complex ventricular arrhythmias: long-term outcome after ablation. *Circulation*. 2013;127:1359–1368. doi: 10.1161/CIRCULATIONAHA.112.000872.
4. Kottkamp H, Wetzel U, Schirdewahn P, Dorszewski A, Gerds-Li JH, Carbucicchio C, Kobza R, Hindricks G. Catheter ablation of ventricular tachycardia in remote myocardial infarction: substrate description guiding placement of individual linear lesions targeting noninducibility. *J Cardiovasc Electrophysiol*. 2003;14:675–681.
5. Jaïs P, Maury P, Khairy P, Sacher F, Nault I, Komatsu Y, Hocini M, Forclaz A, Jadidi AS, Weerasooryia R, Shah A, Derval N, Cochet H, Knecht S, Miyazaki S, Linton N, Rivard L, Wright M, Wilton SB, Scherr D, Pascale P, Roten L, Pederson M, Bordachar P, Laurent F, Kim SJ, Ritter P, Clementy J, Haïssaguerre M. Elimination of local abnormal ventricular activities: a new end point for substrate modification in patients with scar-related ventricular tachycardia. *Circulation*. 2012;125:2184–2196. doi: 10.1161/CIRCULATIONAHA.111.043216.
6. Arenal A, Glez-Torrecilla E, Ortiz M, Villacastín J, Fdez-Portales J, Sousa E, del Castillo S, Perez de Isla L, Jimenez J, Almendral J. Ablation of electrograms with an isolated, delayed component as treatment of unmappable monomorphic ventricular tachycardias in patients with structural heart disease. *J Am Coll Cardiol*. 2003;41:81–92.
7. Yokokawa M, Desjardins B, Crawford T, Good E, Morady F, Bogun F. Reasons for recurrent ventricular tachycardia after catheter ablation of post-infarction ventricular tachycardia. *J Am Coll Cardiol*. 2013;61:66–73. doi: 10.1016/j.jacc.2012.07.059.
8. Yoshida K, Sekiguchi Y, Tanoue K, Endo M, Suzuki A, Kanemoto M, Yamasaki H, Yamauchi Y, Takahashi A, Kuga K, Yamaguchi I, Aonuma K. Feasibility of targeting catheter ablation to the markedly low-voltage area surrounding infarct scars in patients with post-infarction ventricular tachycardia. *Circ J*. 2008;72:1112–1119.
9. Nayyar S, Wilson L, Ganesan AN, Sullivan T, Kuklik P, Chapman D, Brooks AG, Mahajan R, Baumert M, Young GD, Sanders P, Roberts-Thomson KC. High-density mapping of ventricular scar: a comparison of ventricular tachycardia (VT) supporting channels with channels that do not support VT. *Circ Arrhythm Electrophysiol*. 2014;7:90–98. doi: 10.1161/CIRCEP.113.000882.
10. Bogun F, Good E, Reich S, Elmouchi D, Igic P, Lemola K, Tschopp D, Jongnarangsin K, Oral H, Chugh A, Pelosi F, Morady F. Isolated potentials during sinus rhythm and pace-mapping within scars as guides for ablation of post-infarction ventricular tachycardia. *J Am Coll Cardiol*. 2006;47:2013–2019. doi: 10.1016/j.jacc.2005.12.062.
11. Lammers WJ, Kirchhof C, Bonke FI, Allessie MA. Vulnerability of rabbit atrium to reentry by hypoxia. Role of inhomogeneity in conduction and wavelength. *Am J Physiol*. 1992;262(1 Pt 2):H47–H55.
12. Ten Tusscher KH, Panfilov AV. Cell model for efficient simulation of wave propagation in human ventricular tissue under normal and pathological conditions. *Phys Med Biol*. 2006;51:6141–6156. doi: 10.1088/0031-9155/51/23/014.
13. Mickleborough LL, Harris L, Downar E, Parson I, Gray G. A new intraoperative approach for endocardial mapping of ventricular tachycardia. *J Thorac Cardiovasc Surg*. 1988;95:271–280.
14. Mickleborough LL, Usui A, Downar E, Harris L, Parson I, Gray G. Transatrial balloon technique for activation mapping during operations for recurrent ventricular tachycardia. *J Thorac Cardiovasc Surg*. 1990;99:227–32; discussion 232.
15. Mickleborough LL, Mizuno S, Downar E, Gray GC. Late results of operation for ventricular tachycardia. *Ann Thorac Surg*. 1992;54:832–8; discussion 838.
16. Marchlinski FE, Callans DJ, Gottlieb CD, Zado E. Linear ablation lesions for control of unmappable ventricular tachycardia in patients with ischemic and nonischemic cardiomyopathy. *Circulation*. 2000;101:1288–1296.
17. Stevenson WG, Khan H, Sager P, Saxon LA, Middlekauff HR, Natterson PD, Wiener I. Identification of reentry circuit sites during catheter mapping and radiofrequency ablation of ventricular tachycardia late after myocardial infarction. *Circulation*. 1993;88(4 Pt 1):1647–1670.
18. Downar E, Saito J, Doig JC, Chen TC, Sevaptsidis E, Masse S, Kimber S, Mickleborough L, Harris L. Endocardial mapping of ventricular tachycardia in the intact human ventricle. III. Evidence of multiuse reentry with spontaneous and induced block in portions of reentrant path complex. *J Am Coll Cardiol*. 1995;25:1591–1600.
19. Mountantonakis SE, Park RE, Frankel DS, Hutchinson MD, Dixit S, Cooper J, Callans D, Marchlinski FE, Gerstenfeld EP. Relationship between voltage map "channels" and the location of critical isthmus sites in patients with post-infarction cardiomyopathy and ventricular tachycardia. *J Am Coll Cardiol*. 2013;61:2088–2095. doi: 10.1016/j.jacc.2013.02.031.
20. de Bakker JM, van Capelle FJ, Janse MJ, Tasseron S, Vermeulen JT, de Jonge N, Lahpor JR. Slow conduction in the infarcted human heart. 'Zigzag' course of activation. *Circulation*. 1993;88:915–926.
21. Segal OR, Chow AW, Markides V, Schilling RJ, Peters NS, Davies DW. Long-term results after ablation of infarct-related ventricular tachycardia. *Heart Rhythm*. 2005;2:474–482. doi: 10.1016/j.hrthm.2005.01.017.

22. Almendral JM, Gottlieb CD, Rosenthal ME, Stamato NJ, Buxton AE, Marchlinski FE, Miller JM, Josephson ME. Entrainment of ventricular tachycardia: explanation for surface electrocardiographic phenomena by analysis of electrograms recorded within the tachycardia circuit. *Circulation*. 1988;77:569–580.
23. El-Shalakany A, Hadjis T, Papageorgiou P, Monahan K, Epstein L, Josephson ME. Entrainment/mapping criteria for the prediction of termination of ventricular tachycardia by single radiofrequency lesion in patients with coronary artery disease. *Circulation*. 1999;99:2283–2289.
24. Arenal Á, Hernández J, Calvo D, Ceballos C, Atéa L, Datino T, Atienza F, González-Torrecilla E, Eídelman G, Miracle Á, Avila P, Bermejo J, Fernández-Avilés F. Safety, long-term results, and predictors of recurrence after complete endocardial ventricular tachycardia substrate ablation in patients with previous myocardial infarction. *Am J Cardiol*. 2013;111:499–505. doi: 10.1016/j.amjcard.2012.10.031.
25. el-Sherif N, Gough WB, Restivo M. Reentrant ventricular arrhythmias in the late myocardial infarction period: 14. Mechanisms of resetting, entrainment, acceleration, or termination of reentrant tachycardia by programmed electrical stimulation. *Pacing Clin Electrophysiol*. 1987;10:341–371.
26. Segal OR, Chow AW, Peters NS, Davies DW. Mechanisms that initiate ventricular tachycardia in the infarcted human heart. *Heart Rhythm*. 2010;7:57–64. doi: 10.1016/j.hrthm.2009.09.025.
27. Herre JM, Mann DE, Luck JC, Magro SA, Figali S, Breen T, Wyndham CR. Effect of increased current, multiple pacing sites and number of extrastimuli on induction of ventricular tachycardia. *Am J Cardiol*. 1986;57:102–107.
28. Kay GN, Epstein AE, Plumb VJ. Region of slow conduction in sustained ventricular tachycardia: direct endocardial recordings and functional characterization in humans. *J Am Coll Cardiol*. 1988;11:109–116.
29. Cabo C, Pertsov AM, Baxter WT, Davidenko JM, Gray RA, Jalife J. Wave-front curvature as a cause of slow conduction and block in isolated cardiac muscle. *Circ Res*. 1994;75:1014–1028.
30. Gilbert SH, Benson AP, Walton RD, Bernus O. Slowed propagation across the compacta-trabeculata interface: a consequence of fiber and sheet anisotropy. *Conf Proc IEEE Eng Med Biol Soc*. 2011;2011:1688–1692. doi: 10.1109/IEMBS.2011.6090485.
31. Irie T, Yu R, Bradfield JS, Vaseghi M, Buch EF, Ajijola O, Macias C, Fujimura O, Mandapati R, Boyle NG, Shivkumar K, Tung R. Relationship between sinus rhythm late activation zones and critical sites for scar-related ventricular tachycardia: systematic analysis of isochronal late activation mapping. *Circ Arrhythm Electrophysiol*. 2015;8:390–399. doi: 10.1161/CIRCEP.114.002637.

Circulation
Arrhythmia and Electrophysiology

Decrement Evoked Potential Mapping: Basis of a Mechanistic Strategy for Ventricular Tachycardia Ablation

Nicholas Jackson, Sigfus Gizurarson, Karthik Viswanathan, Benjamin King, Stephane Massé, Marjan Kusha, Andreu Porta-Sanchez, John Roshan Jacob, Fakhar Khan, Moloy Das, Andrew C.T. Ha, Ali Pashaei, Edward Vigmond, Eugene Downar and Kumaraswamy Nanthakumar

Circ Arrhythm Electrophysiol. 2015;8:1433-1442; originally published online October 19, 2015;
doi: 10.1161/CIRCEP.115.003083
Circulation: Arrhythmia and Electrophysiology is published by the American Heart Association, 7272 Greenville Avenue, Dallas, TX 75231

Print ISSN: 1941-3149. Online ISSN: 1941-3084